

# Geophysical prospecting with controlled-source electromagnetic data

Author: Oriol Roqué Paniagua.

*Facultat de Física, Universitat de Barcelona, Diagonal 645, 08028 Barcelona, Spain.*

Advisor: Dr. Alex Marcuello

**Abstract:** Controlled-source electromagnetics (CSEM) is an active geophysical technique sensitive to the electrical resistivity of the subsoil, with the peculiarity that the source producing the electromagnetic signal is a man-made device. It has been largely applied for offshore environments in hydrocarbon exploration due to the good penetration depth and resolution, although its application onshore is still under investigation because it is less favorable. In order to study this technique, a dataset was acquired at Samalús (Vallès Oriental) the 22<sup>nd</sup> and 23<sup>rd</sup> February, 2017; and in this work a 1D model simulation and interpretation of these data is presented.

## I. INTRODUCTION

CSEM is an electromagnetic (EM) technique that consists in the generation by a transmitter of an EM signal that propagates through the subsoil until it reaches a receiver, which measures the electric field that has been modified because of the presence of the media. Among the different physical properties, the electrical resistivity is the most relevant parameter to characterize the subsoil with this technique. It quantifies the resistance of certain materials to the flow of electric current through them and its inverse corresponds to electrical conductivity. It depends mainly on porosity and pore structure of the rock, and on the content, salinity and saturation of the fluids inside. Typical values of resistivity of rocks range between 1 to  $10^4 \Omega\text{m}$ , although more extreme values are possible in mineral ores ( $10^{-5} \Omega\text{m}$ ) and crystalline rocks ( $10^6 \Omega\text{m}$ ) [1].

In a wide sense, electromagnetic methods can be divided into passive methods, which are characterized by the use of natural currents or fields to obtain information, and active methods, which ensure high amplitude of the signal by producing it with a man-made source. Their difference in use relies mostly in the range of depth to be explored and the quality of the data that will be obtained. For instance, an active method is electrical resistivity tomography (ERT) and a passive one is magnetotellurics (MT). ERT covers depths in the order of tens of meters, while MT reaches much higher depths, from hundreds of meters to tens of kilometers [2].

CSEM produces data with a large signal-to-noise ratio because of the man-made source [3]. Consequently, it might theoretically be a capable technique for both exploration geophysics and monitoring of reservoirs. For the second purpose it is needed a sensitivity much larger than experimental uncertainties, besides a fine accuracy and repeatability of measurements [3]. However, the main application of CSEM relies on the detection of hydrocarbon deposits in marine environment, which in general are more resistive than saline water. The method shows a greater signal-to-noise ratio and penetration depth in the marine scenery rather than onshore environments because the ocean acts as a low pass filter for EM natural

signals from the ionosphere and magnetosphere, enhancing the quality of the data obtained [4]. Simple simulations have shown that detecting resistors is more challenging than detecting conductors in a resistive surrounding due to the fact that currents flow mainly in conductive structures [5]. However, the visibility of the particular structure depends on the configuration and disposal of the transmitter and receiver stations, besides the type of EM field measured.

To gain experience in this technique, I participated in a fieldwork in the NW boundary of the Vallès basin conducted by the Department of Earth and Ocean Dynamics. The aim of this study is to obtain a 1D geoelectrical model of the ground using some of the data collected there with the CSEM technique.

## II. METHODOLOGY

Among the different device configurations between transmitter and receivers, an array of receivers and the source located at the same surface is considered in this work (Fig. 1). This array is called surface-to-surface configuration. Other configurations including a transmitter or receivers in boreholes are also possible, but are beyond this study. Particularizing in the surface-to-surface configuration and considering the devices as electric dipoles, if both receiver and transmitter dipoles are aligned, it is referred as inline mode (1). If these dipoles are perpendicular to the line that connects them, it is named broadside mode (2). Other options exist in which the source can be a magnetic dipole, e.g. a vertical magnetic dipole generated by a horizontal current loop (3).

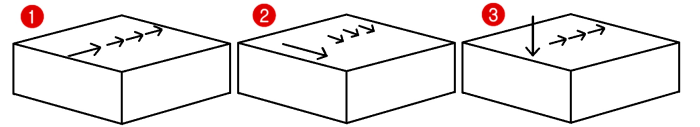


FIG. 1: Surface-to-surface configurations: (1) Inline electric dipole. (2) Broadside electric dipole. (3) Vertical magnetic dipole. All devices are assumed to be dipoles. The largest arrow indicates the source and the rest the receivers.

This work focuses in the inline electric dipole configuration with a surface-to-surface emission (1). Both types of devices are approximated as electric dipoles: receivers measure the difference in electric potential between their two electrodes in a given position; meanwhile the source emits an EM signal provided by the injection of electric current between its electrodes, which is achieved with an external power supply. In general, the dipole of the source is larger than the dipole of the receiver. It can be shown that a surface-to-surface configuration with a dipole horizontally orientated allows getting data with larger amplitude of the electric field, which is clearly an advantage in inland CSEM because of the attenuation of the signal. This fact is attributed to a guided-wave EM mode inside the resistive body between conductive layers [5].

The use of low frequency signals in CSEM allows the simplification of the displacement current on the propagation equations. Magnetic susceptibility is also considered negligible for most common geologic materials. Assuming a homogeneous media, the expression for the component of the electric field along  $x$  by the emission of an  $x$ -oriented infinitesimal dipole is [6]:

$$E_x(x) = \frac{I\rho ds}{2\pi x^3} \exp^{-ikx}(1 + ikx), \quad (1)$$

where  $I$  is the electric current,  $ds$  is the length of the dipole,  $\rho$  is the resistivity and  $k$  is the propagation constant, which reads:

$$k^2 = -i \frac{\omega\mu_0}{\rho}, \quad (2)$$

where  $\omega$  is the angular frequency and  $\mu_0$  is the magnetic permeability of the vacuum. The source moment is defined as  $J = Ids$  and contains all parameters related to the transmitter. The dipole approximation is valid if the observation point is at least 5 source dipole-lengths away from the center of it [6].

There are three main factors that can modify the signal intensity: due to the configuration of the source as a dipole, it is expected a geometric spreading of the amplitude of the electric field from the source proportional to  $x^{-3}$  as stated in Eq. (1). If the signal crosses a boundary between two layers of different resistivity, the electric field amplitude must be discontinuous in order to ensure the continuity of the normal component of the electrical current density. This process generates the called galvanic effect. Finally, conductive materials attenuate the EM signal because the propagation constant is a complex number (Eq. 2).

Notice that receivers cannot be localized neither too close to the source nor too away from it, because data would only reproduce the transmitter signal or the signal strength would be too low, respectively. The extent in depth to which an electromagnetic signal might penetrate before it attenuates can be easily characterized by the skin depth. It corresponds to the depth where the amplitude of a plane wave decays by a factor of  $e$  and

depends on the frequency of the signal, resistivity and magnetic permeability:

$$\delta = \sqrt{\frac{2\rho}{\omega\mu_0}}. \quad (3)$$

Therefore, a high frequency implies a decrease in the reach of the penetrating signal, as well as a media composed by low resistivity geological structures. In general, in geophysics surveying, a high separation of source and receivers allows getting data from deeper conductive structures. Typical values of penetration using CSEM method are in the range between several tens of meters up to few kilometers.

The process to characterize the subsoil starts with the data collected by receiver stations. The electric field at the receiver can be calculated by dividing its potential difference by the length of the dipole. Since the dipole is not infinitesimal, it is considered that the value obtained of the field corresponds to the value it would have the midpoint in length of the receiver. This measure is mainly the original time-domain signal altered by the effect of subsoil conductivity distribution, besides external factors affecting it in the shape of noise. The signal produced by the transmitter is also recorded in order to obtain the shape and time of source moment. When modeling the subsoil as a linear system, in which a signal in enters and a signal out leaves it, we can calculate the transfer function  $T$ , which provides information about resistivity properties [3]. The relation between these variables is the following:

$$E_r(x, t) = T(x, t)J(t). \quad (4)$$

This perception allows the utilization of the Fourier transform in order to change the time-domain data to frequency-domain. Theoretically, both domains contain the same amount of information, although in the frequency domain noise can be filtered [6]. The amplitude of this transfer function is the variable that acts as the impedance in the medium, and must be adjusted by ground profiles simulation. Since CSEM uses a man-made source, it is possible to change the fundamental frequency of each emission to enhance the further data treatment.

### III. DATA ACQUISITION AND PROCESSING

The exploration was performed in Samalús, in the NW of the Vallès basin. A MT profile was already effectuated in 2014 in the same zone [7]. A previous plan of the experiment was provided in order to make the process on the field more agile. It contained a list of all items needed for the exploration, the position of the stations on the profile line and the different emissions to perform. However, two stations had to be located on a different position due to the impossibility of access, resulting in a modified profile line (Fig. 2).

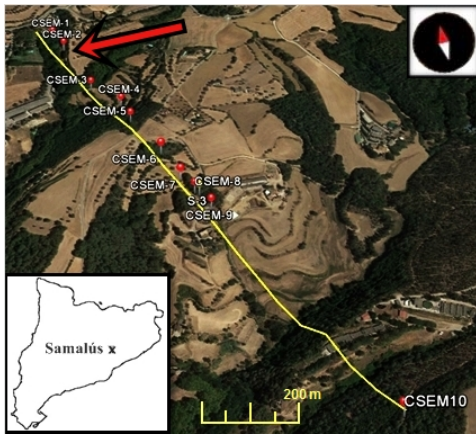


FIG. 2: Location of the profile line of CSEM exploration in Samalús. The arrow shows the place of the emission studied.

The original set up consisted in a straight line shaped array of 10 Wordsensing SRU Spider data loggers as receiver stations and a source composed of the Zonge equipment ZT-30 ZeroTEM transmitter and XMT-G transmitter controller (Fig. 3). Since a good degree of correlation is needed between signals, it is essential to have an accurate localization of each site. Therefore, a GPS device was equipped in all stations. Each receiver was a dipole of 15-20 m oriented along the direction  $335^\circ$  E, with a sample frequency of 500 Hz. All electrodes were made of stainless steel. The source transmitter was a dipole of 34-70 m length and the electric current was supplied by a set of ten 12 V car batteries. The transmitter signal was characterized by a SRU Spider connected to the ZT-30 Zero TEM transmitter. Using a computer, collected data could be visualized *in situ*, in order to guarantee the correct operation of the station, for both source and receiver devices. In this experiment, the criterion of polarity chosen was to take the northern electrode as the negative. The original plan was to transmit at 5 different fundamental frequencies during a time lapse predetermined: 0.125, 0.5, 2, 8 and 32 Hz. Unfortunately, the emission of the highest frequency could not be realized in the field because of some technical problems. Since the EM signal was a square wave, odd harmonics of these fundamental frequencies could be also recorded. Three surface-to-surface emissions were produced at 2<sup>nd</sup>, 8<sup>th</sup> and 10<sup>th</sup> sites, and a single Long Electrode Mise-à-la-Masse (LEMAM) emission was also performed. It consisted in taking advantage of a well that was of special interest in the 8<sup>th</sup> station site and using the metallic casing of the well as one of the electrodes of the source.

This study focuses in a particular dataset, the one that consisted of the inline surface-to-surface emission corresponding to 2<sup>nd</sup> station site (Fig. 2). This means that the first site corresponding to the first receiver is contrary located to the source if compared with the 3<sup>rd</sup> to 10<sup>th</sup> sites, which correspond to the 2<sup>nd</sup> to 9<sup>th</sup> receivers, respectively. However, a positive array of receivers conserving the rel-



FIG. 3: Devices composing the source station: (1) Batteries. (2) XMT-G transmitter controller. (3) ZT-30 ZeroTEM transmitter. (4) Box containing SRU Spider data logger and GPS. (5) Computer.

ative distance between them has been considered since no difference in the result would appear in a 1D data interpretation with a layered structure. In this emission, the length of the emission dipole was of 34 m and the contacts showed a resistance of  $85.8 \Omega$ . GPS system provided the location of each station in geographic Cartesian coordinates, which have been rescaled to a straight line corresponding to the array of stations, with the origin lying on the emission site.

Time-domain field data have been processed and transformed to frequency-domain by the software developed at Department of Earth and Ocean Dynamics. The processed data they provided was the amplitude of the transfer function for the 34 frequencies and the 9 receiver stations, each one with its uncertainty (Fig. 4). In general, the amplitude decreases strongly with the distance to the source. However, data concerning the 7<sup>th</sup> receiver shows an increase in amplitude despite this tendency, regardless of the frequency. This behavior is due to the fact that one of the electrodes used in this receiver dipole was the metallic casing of the exploration well. This conductive structure allows the signal to be propagated more effectively to the surface [3]. Finally, data uncertainties are normally higher for those harmonics produced by the lowest frequency.

#### IV. MODELING

The geological structure in this area is expected to be horizontally stratified [7], and the 1D modeling of the data acquired can offer an image of it. The code selected for modeling a 1D EM structures is free available and named Dipole1D [8]. In this work, I used the version found at the Web Hosted Active-source Modeling (WHAM) [9].

It returns the Cartesian components of the electromagnetic fields at the positions where receivers are located,

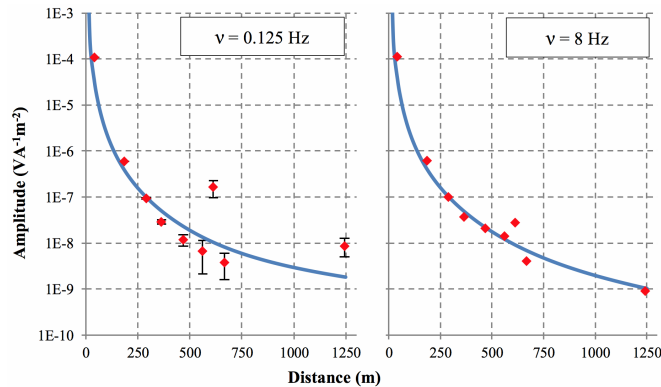


FIG. 4: Amplitude of the transfer function vs. distance at 0.125 Hz (left) and 8 Hz (right) for both experimental data (red) and selected model (blue).

assuming an infinitesimal electric dipole acting as the source of the signal. The program allows the definition of plane-parallel layers of different isotropic resistivity; in fact, an air layer has to be considered as well. Assuming a harmonic time variation of the fields, the code computes the magnetic potential vector by means of the Henkel transform equation at every point. With this information, the EM fields can be easily calculated. The theoretical development can be found in [8]. Since transmitter and receivers can be placed anywhere, multiple distributions can be simulated. It is only needed to specify these localizations in the case of interest, the frequency at which the signal propagates and the maximum spatial range. A first estimation of the subsoil was provided by the previous geophysical study [7], which allowed the restriction of the variables in a certain range.

In particular, modeling has been focused into a two layer model in order to get a first approximation of the electrical resistivity of the subsoil. The air layer is assumed constant and is characterized by having a resistivity of  $10^{12} \Omega m$ . A trial-and error scheme was used to obtain the model. A total of 27 models have been simulated with the 4 fundamental frequencies, and selected models with the entire pack of 34 frequencies. In order to be able to compare the quality of a model, the following logarithmic normalized RMS has been considered:

$$RMS = \sqrt{\frac{1}{N-1} \sum_{i=1}^N \left( \frac{\Delta \ln T}{\epsilon} \right)^2}, \quad (5)$$

where  $N$  is the number of data,  $T$  is the amplitude of the transfer function and  $\epsilon$  takes into account the data field uncertainty. The logarithmic approach has been used in order to rescale the widely separated values obtained in the amplitudes of the transfer function (Fig. 4). Keep in mind that for small variations  $\Delta \ln |T| = \Delta |T|/|T|$ . The selected model consists of a two layer model: a superficial layer with a resistivity of  $8 \Omega m$ , which is a more conductive ground than the deepest one, with a  $1000 \Omega m$ . A thickness of 450 m is assumed for

the shallow layer, while the second is supposed to be infinite halfspace. The RMS of this model is 3.45, and the respective RMS of each station can be visualized in the following table:

Station	$R_1$	$R_2$	$R_3$	$R_4$	$R_5$	$R_6$	$R_7$	$R_8$	$R_9$
RMS (%)	5.77	2.26	0.70	1.35	1.24	1.79	6.55	3.08	3.47

TABLE I: Logarithmic normalized RMS for each receiver station.

Finally, both treated field data and the results provided by this model can be seen in Fig. 5.

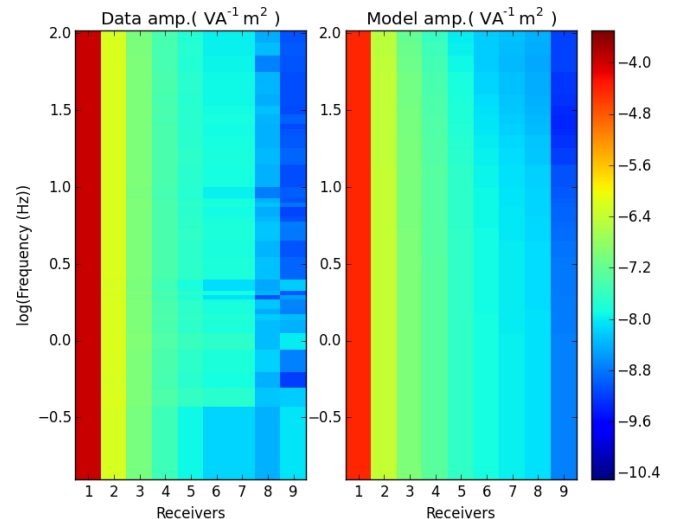


FIG. 5: Amplitude of the transfer function for each receiver at a certain frequency for the data and the selected model.

## V. DISCUSSION

In order to quantify the differences between experimental data and the values predicted by the model, the relative discrepancy of the logarithm of each value has been calculated (Fig. 6).

Clearly the 7<sup>th</sup> receiver shows the worst fitting due to the use of the metallic casing of the well as an electrode. Considering that a lateral change of resistivity cannot be taken into account in a 1D model, the theoretical values concerning this site will not reproduce the data. Besides, the 1<sup>st</sup> receiver is too close to the transmitter. Under this circumstance, the approximation of uniform  $E$  field, that is to say, assuming the expected electric field value as the value that the electric field would have on the middle of the dipole of the receiver might not be accurate. This approximation is assumed for the data processing because it allows an easy treatment and does not affect on large distances. Finally, the last receiver presented the worst signal-to-noise ratio since it is the farthest. Therefore,



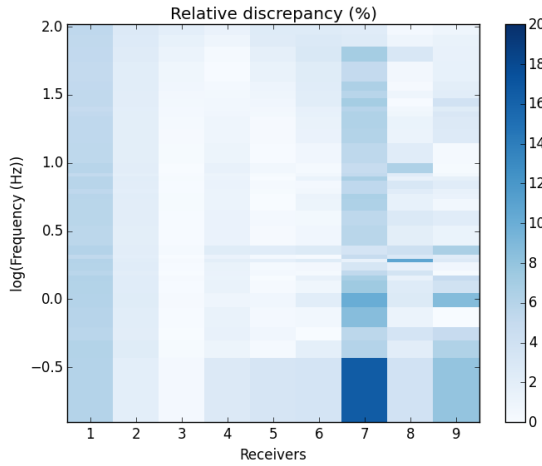


FIG. 6: Relative logarithmic discrepancy between treated experimental data and the results of the model.

the data of this receiver have higher uncertainty than the rest of the stations and different models can be consistent with them. It can also be observed that the behavior of the transfer function shows slightly less discrepancy at higher frequencies rather than low frequencies. However, model responses and data coincide in a medium range of distances, for both high and low frequencies. This model is consistent with the results of the previous study due to the restriction of the variables on the modeling.

Finally, notice that different strategies for modeling could be adopted, e.g., by fitting data of a single receiver station with a two layer model, resulting in 9 different layered structures of different resistivity and thicknesses. The overall 1D model would be obtained by averaging the results, with an uncertainty achieved by taking into account the adjustment error of each model and the deviation of them from the mean one. However, this strategy might be also an approach to introduce lateral changes in the layered model.

## VI. CONCLUSIONS

- Despite being a technique mostly implemented in the marine environment, CSEM can be used on some inland applications such as geophysical surveying. In particular, this work focuses in a CSEM prospecting in Samalús in which I participated. In regard to the experimental data obtained from an inline surface-to-surface configuration, a preliminary electrical model of the ground has been developed and discussed. It resulted in a two layer model with a superficial layer of  $8 \Omega\text{m}$  and 450 m thick, and a deeper layer of  $1000 \Omega\text{m}$ . Furthermore, it has been shown that the result is consistent with the previous geophysical study in the same area.
- However, some limitations in the model shall be considered. These are mainly because of using 1D modeling; each simplification turns into an easier problem to be resolved although it restrains the quality of the solution. Besides, the lack of a compiled version of the modeling program limits the option to enhance the velocity of the modeling process results, and only few models have been explored. More layers could also be added to the model to get a finest adjustment if the previous problem had been solved.

## Acknowledgments

I would like to give my sincere gratitude to Alex Marcuello for his guidance and motivation while working in this project. I also would like to thank the Department of Earth and Ocean Dynamics (UB) to allow me to participate in the fieldwork and all the help they provided. Finally, special thanks to my family, to my colleagues for their collaboration, to David for his ideas and to Sara for always being there.

- 
- [1] Lowrie, W., *Fundamentals of Geophysics*, (Cambridge University Press, Cambridge, 2007).
  - [2] Dentith, M. T. & Mudge, S., *Geophysics for the mineral exploration Geoscientist*, (Cambridge University Press, Cambridge, 2015).
  - [3] Vilamajó, E., "CSEM monitoring at the Hontomín CO<sub>2</sub> storage site: modeling, experimental design and baseline results". PhD thesis (2016).
  - [4] Mehta, K., Nabighian, M. N. & Li, Y., "Controlled Source Electromagnetic (CSEM) technique for detection and delineation hydrocarbon reservoirs: an evaluation". SEG Technical Program Expanded Abstracts: pp. 546-549 (2005).
  - [5] Streich, R., "Controlled-Source Electromagnetic Approaches for Hydrocarbon Exploration and Monitoring on Land". *Surveys in Geophysics* **37**: 47-80 (2016).
  - [6] Nabighian, M. N., ed. *Society of Exploration Geophysicists, Electromagnetic methods in applied geophysics*, (Tulsa, 1987).
  - [7] Geomodels UB, "Realització de treballs de camp per a l'adquisició de dades magnetotellúriques i treballs de modelització i interpretació geofísica 3D (inversió 3D de les dades) per l'estudi d'estructures geològiques profundes en dues àrees de Catalunya: La Garriga (Vallès Oriental) i el Baridà (Alt-Urgell-Cerdanya)". ICGC technical report, pp. 200 (2016).
  - [8] Key, K., "1D inversion of multicomponent, multifrequency marine CSEM data: Methodology and synthetic studies for resolving thin resistive layers". *Geophysics*, **74**(2): 9-20 (2009).
  - [9] Key, K., "Web Hosted Active-source Modeling" (Accessed in March 2017). <http://marineemlab.ucsd.edu/wham/>